iScience

CellPress
OPEN ACCESS

Article

Differential alternative splicing landscape identifies potentially functional RNA binding proteins in early embryonic development in mammals

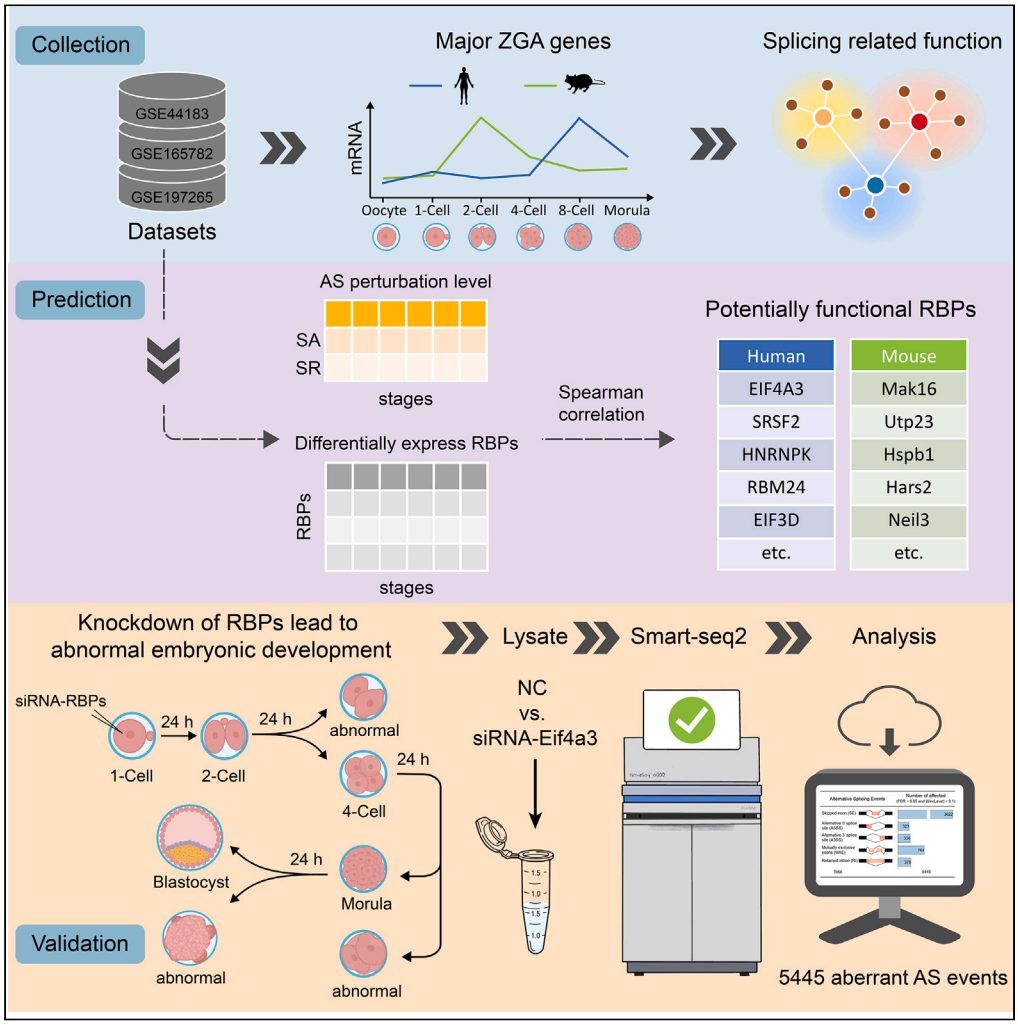

Jianhua Chen, Yanni He, Liangliang Chen, ..., Na Li, Congxiu Miao, Ruizhi Feng

mcxms@163.com (C.M.)
ruizhifeng@njmu.edu.cn (R.F.)

Highlights

Maternal-to-zygotic transition was closely related to alternative splicing

A pipeline to predict potentially functional RNA binding proteins was developed

EIF4A3, MAK16, SRSF2, and UTP23 were associated with reproductive disorders

Eif4a3-knockdown embryos failed to develop normally because of aberrant splicing

Chen et al., iScience 27, 109104
March 15, 2024 © 2024
https://doi.org/10.1016/j.isci.2024.109104

iScience

CellPress
OPEN ACCESS

Article

Differential alternative splicing landscape identifies potentially functional RNA binding proteins in early embryonic development in mammals

Jianhua Chen,[1,4] Yanni He,[1,4] Liangliang Chen,[1] Tian Wu,[1] Guangping Yang,[1] Hui Luo,[1] Saifei Hu,[1] Siyue Yin,[1] Yun Qian,[2] Hui Miao,[3] Na Li,[3] Congxiu Miao,[3,*] and Ruizhi Feng[1,2,5,*]

SUMMARY

Alternative splicing (AS) as one of the important post-transcriptional regulatory mechanisms has been poorly studied during embryogenesis. In this study, we comprehensively collected and analyzed the transcriptome data of early embryos from human and mouse. We found that AS plays an important role in this process and predicted candidate RNA binding protein (RBP) regulators that are associated with reproductive development. The predicted RBPs such as EIF4A3, MAK16, SRSF2, and UTP23 were found to be associated with reproductive disorders. By Smart-seq2 sequencing analysis, we identified 5445 aberrant alternative splicing events in Eif4a3-knockdown embryos. These events were preferentially associated with RNA processing. In conclusion, our work on the landscape and potential function of alternative splicing events will boost further investigation of detailed mechanisms and key factors regulating mammalian early embryo development and promote the inspiration of pharmaceutical approaches for disorders in this crucial biology process.

INTRODUCTION

Maternal mRNAs storing in the oocyte are mostly translational inactivated.[1] After fertilization, these mRNAs are heavily translated into proteins that play important roles in early embryo development.[2] As development proceeds, the embryonic/zygotic genome activates, maternal factors degrade and the embryo becomes dependent on the its genome expression maintaining vital activities. This is a process known as maternal-to-zygotic transition (MZT).[3] It has been found that the clearance of maternal factors is mediated by both the maternal-decay (M-decay) and zygote-decay (Z-decay) pathways[4] and dysregulation of this process is associated with various reproductive diseases such as early developmental arrest and oocyte maturation disorder.[3,5–7] In studies of embryonic/zygotic genome activation (EGA/ZGA), it is generally accepted that after a smaller minor wave of ZGA, comes the first major wave of transcription, the major ZGA, and it occurs at different developmental stages in different species.[8,9] For example, in mice occurs at the 2-cell period, whereas in humans, large-scale embryonic gene activation takes place at the 8-cell stage,[10–12] implying intrinsic developmental differences between species. However, most current studies on maternal factor degradation and ZGA at the transcriptional level are limited to gene expression analysis.[4,6,7]

As an important manner of post-transcriptional regulation, only a handful of studies have focused on alternative splicing (AS) events at the embryonic developmental stage, and its potential function in ZGA and early embryo development is largely unraveled. For instance, a novel splice isoform was identified in hydroxysteroid 17-beta dehydrogenase 3 (Hsd17b3) gene in pig testis. The isoform had a deletion in the 5′ UTR region and is significantly associated with porcine reproductive traits.[13] In another research, the estrogen receptor alpha variant Δ7 (ERΔ7), produced by AS in the female myometrium, act as a regulator of myometrium quiescence and may promote fetal development.[14] In studies comparing mature and immature human oocytes, genes with altered AS patterns were found to be primarily associated with metabolism and cell cycle, suggesting that AS may be a candidate mechanism for managing oocyte maturation.[15] Prevalent splicing events have been found during preimplantation embryonic development in some studies,[16–19] but the molecular mechanisms regulating these events are still poorly understood. One potential hypothesis was proposed that alterations in AS events may be regulated by *cis*-acting elements, *trans*-acting factors, transcriptional factors and epigenetic factors. Luping Yu et al. found that loss of epithelial splicing regulatory protein 1 (Esrp1) interfered with a series of genetic splicing sites, which may lead to abnormal spindle organization in oocytes and female infertility.[20] Given that most of these *trans*-acting factors are RNA binding proteins (RBPs), systematic identification of potential target RBPs would find more *trans*-acting factors that play a

[1]State Key Laboratory of Reproduction Medicine and Offspring Health, Nanjing Medical University, Nanjing, Jiangsu 210029, China
[2]Reproductive Medical Center of Second Affiliated Hospital of Nanjing Medical University, Nanjing, Jiangsu 210008, China
[3]Department of Reproductive Genetics, Heping Hospital of Changzhi Medical College, Key Laboratory of Reproduction Engineer of Shanxi Health Committee, Changzhi, Shanxi 046000, China
[4]These authors have contributed equally
[5]Lead contact
*Correspondence: mcxms@163.com (C.M.), ruizhifeng@njmu.edu.cn (R.F.)
https://doi.org/10.1016/j.isci.2024.109104

significant role in preimplantation biological processes. We hypothesize that the level of AS can reflect the potential function of RBPs. However, there is a lack of bioinformatic and experimental pipeline to identify these crucial regulators in early embryo development.

In order to identify RBP regulatory candidate genes in early embryo development, we comprehensively collected transcriptome data from mouse and human oocytes and early embryos to dissect the global pattern of gene expression and AS. We developed a bioinformatic approach utilizing AS events to identify vital RBP regulators during preimplantation embryo development. We then investigated the predicted regulators whose function were little known in the reproductive system by knocking down their expression in zygotic mouse embryos. Together, this study provides help in revealing molecular mechanisms for better understanding of the post-transcriptional regulation in early embryo development.

RESULTS

The global transcriptional pattern found the critical stage in early embryonic development in human and mouse

Firstly, single-cell transcriptome sequencing data at various stages of human and mouse preimplantation embryos were collected as shown in Methods. For the utilization of rMATS, it is necessary to have samples with the same read length. Thus, we abandoned four human 8-cell samples (49 bp) and the rest samples (90 bp) were analyzed for the downstream procedures. On average, 15.8 million reads were detected per human sample and 12.3 million reads per mouse sample. The unique mapping rates were 92.8% for human samples and 83.9% for mouse samples (Table S1).

Different gene expression levels were divided according to the FPKM threshold. Overall, in both human and mouse data, the total number of transcripts at the 1-cell stage peaks after sperm and eggs combine, and then drops rapidly at the 2-cell stage (Figures 1A and S1A, detailed data shown in Tables 1 and 2). This is also consistent with previous studies showing that degradation of the maternal mRNA pool is one of the mechanisms driving the switch from oocyte to embryo development.[8,21] In the lower expression level of $0 < FPKM \leq 1$, the number of transcripts in the six developmental stages had the same trendline of change with all transcripts. In human data, transcripts number increased gradually from 2-cell to morula. In mouse, the number decreased form 2-cell to 8-cell, and increased from 8-cell to morula. In both species, the number of transcripts with lower expression ($0 < FPKM \leq 1$) showed a sharp increase from 8-cell to morula (dark blue line in Figures 1A and 1B). When comparing the number of transcripts in different group of expression level during early embryo development, we found that the number of transcripts in the human 8-cell stage was the highest among the low ($1 < FPKM \leq 10$), medium ($10 < FPKM \leq 100$) and high (FPKM >100) expression groups except for the 1-cell stage (Figure 1A). The number of mouse 2-cell stage transcripts was the highest in the low ($1 < FPKM \leq 10$) and medium ($10 < FPKM \leq 100$) expression group, while the number of mouse 2-cell stage transcripts was the least in the high (FPKM >100) expression level (Figure S1A). Differentially expressed genes (DEGs, padj<0.05 & $|\log_2 FoldChagne| > 2$) between each adjacent stage were shown with color shades, indicating the range of values of $\log_2 FoldChange$ (Figures 1B and S1B). We found that the maximum count of up-regulated DEGs in human samples was between 4-cell and 8-cell stages (4289 DEGs, 2955 up, 1334 down) and in mouse samples was between 1-cell and 2-cell stages (6133 DEGs, 3076 up, 3057 down). In human, though oocyte to 1-cell has the most DEGs (4304 DEGs, 596 up, 3708 down), the majority of them are down-regulated genes. Interestingly, down-regulated genes in 1-cell to 2-cell were more than those in oocyte to 1-cell (2084 DEGs, 395 up, 1689 down) in mouse.

Whereas the MZT requires the clearance of maternal products and the activation of zygotic genome (ZGA). ZGA is not a single event, but a period in which transcription is gradually activated. In the low and medium expression group, both human and mouse experienced a transcript surge at the 1-cell stage, followed by a peak at the 8-cell in human and 2-cell in mouse, and the whole process changed dynamically. All these discoveries are consistent with the previous research, which suggest the first major wave of transcription (zygotic or embryonic genome activation, ZGA/EGA) after a smaller minor wave occurs in the totipotent mouse 2-cell and human 8-cell embryo.

Clustering of global gene expression patterns

The global gene expression patterns were identified in mouse and human respectively by cluster using the fuzzy c-means algorithm. Complete clustering plot can be checked in Data S2 (human) and Data S3 (mouse). According to the programmed waves, we categorized the clusters as maternal RNA, minor ZGA and major ZGA. The maternal RNA pattern is that the gene expression level decreases after the oocyte. The expression pattern of minor ZGA in both human and mouse reached a peak at the 1-cell stage following declined. The major ZGA pattern in human was different from that in mouse. Human major ZGA reached its peak at 8-cell stage, while mouse reached its peak at 2-cell stage. As shown in Figures 1C and S1C, human major ZGA contains more genes than the minor ZGA and maternal RNA, in contrast to the mouse major ZGA which contains fewer genes than both the minor ZGA and maternal RNA. This suggests that the human embryonic genome activation process is much more complex than that of the mouse. Looking at the expression levels of these genes throughout developmental stages (Figures 1D and S1D) revealed that maternal RNA involves genes with higher average expression than both minor ZGA and major ZGA. This indicates that maternal factors play an important function in early embryonic development. It is amazing that the expression levels of the genes involved in minor ZGA are overall higher than those involved in major ZGA, hints that although many studies have focused on the role of major ZGA, minor ZGA is also crucial for embryonic development.

Splicing regulation is important during human major ZGA

Subsequently, we performed a gene ontology (GO) enrichment analysis of the genes contained in the major ZGA using Metascape website. We can get a rough look at the biological process via the parent GO terms. As shown in Figure 1E, each parent GO term contains multiple

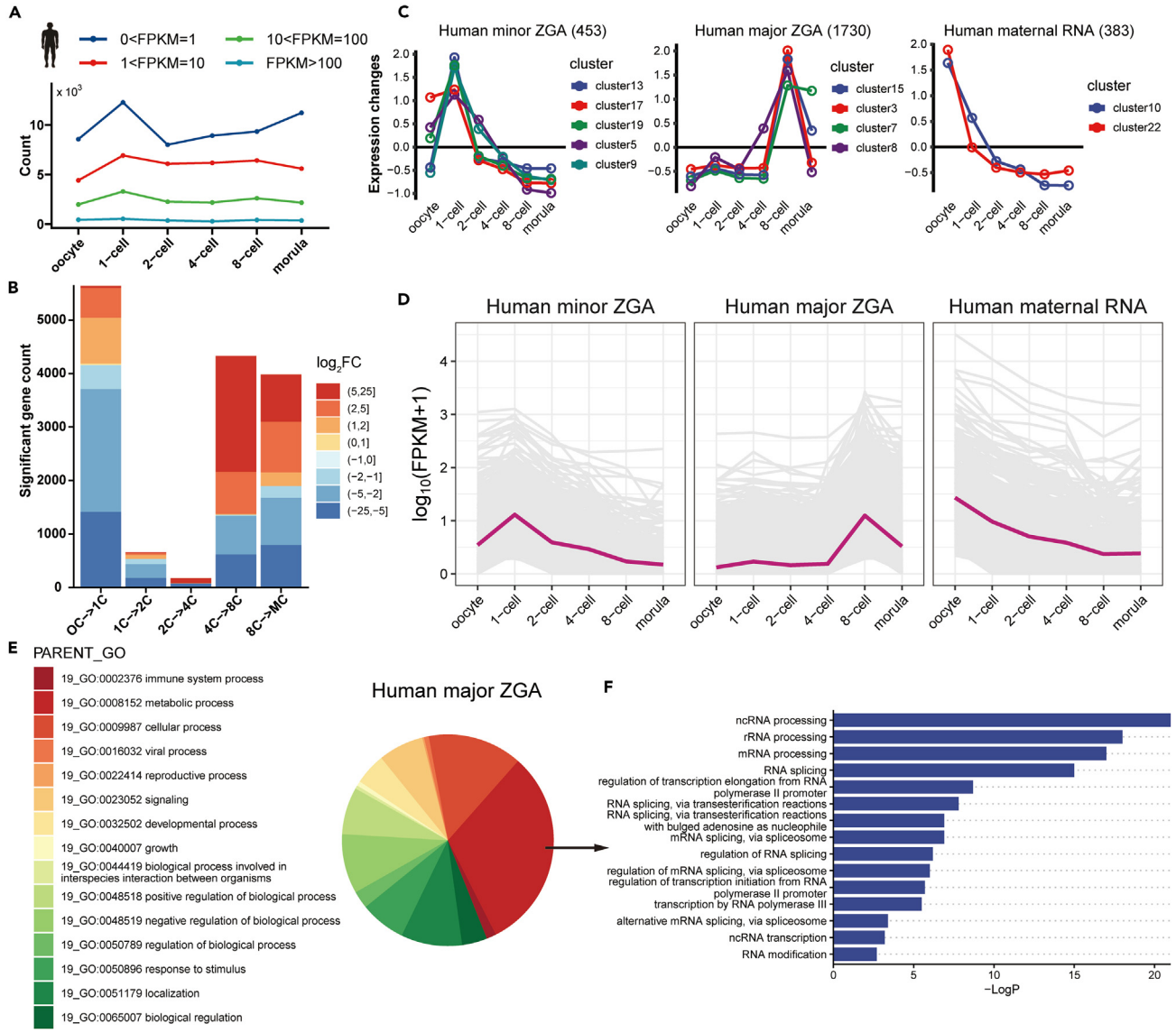

Figure 1. Global description of transcriptome profiles in human early embryonic development

(A) Statistical graph of the number of different classifications of gene expression.

(B) Distribution of log_2FoldChagne value of gene expression between consecutive two stages, the genes with padj<0.05 and $|log_2FoldChange|>2$ are defined as differentially expressed genes (DEGs).

(C) Cluster of maternal RNA, minor ZGA, and major ZGA related genes, which were obtained by fuzzy C-means clustering. x lab means different developmental stage over time, y lab represents the average expression level of the clustered genes.

(D) Line chart exhibits the expression level of human minor ZGA, major ZGA, and maternal RAN-related genes throughout the embryo development. Each gray line represents one gene; the carmine line is the mean value of the expression.

(E) Proportion of parental terms of each term for functional enrichment analysis of human major ZGA related genes.

(F) Entries that belong to metabolic process in human major ZGA.

specific child GO terms, the human major ZGA-related genes were enriched for 15 parent GO terms, mainly for metabolic process (GO:0008152) and cellular process (GO:0009987), but also for some developmental processes, such as reproductive process (GO:0022414), growth (GO:0040007) and developmental process (GO:0032502). In addition to these, immune and stimulation related processes are also involved. In the parent term metabolic process, which contains the most child GO terms, majority of the terms are related to RNA metabolism and involve multiple processes that regulate mRNA splicing and modification (Figure 1F), suggesting that splicing may perform an important function in the regulation of early human embryonic development. This process may be linked not only to the different spliceosomes themselves, but also to various proteins that regulate splicing behavior. Surprisingly, enrichment analysis of mouse

Table 1. The number of transcripts during the six developmental stage in human

	oocyte	1-cell	2-cell	4-cell	8-cell	morula
0<FPKM≤1	8564	12275	8005	8924	9339	11225
1<FPKM≤10	4413	6920	6086	6177	6418	5597
10<FPKM≤100	1977	3290	2257	2176	2604	2161
FPKM>100	435	526	361	277	411	360
Sum	15389	23011	16709	17554	18772	/

major ZGA-associated genes showed different results than in human, and although it also had a large number of terms belonging to metabolic processes (Figure S1E), these entries were mainly associated with histone modification and methylation (Figure S1F). Instead, multiple of terms were enriched in pathways related to the immune system process (GO:0002376). This suggests that the mechanism of mouse major ZGA differs from that of human and may involve processed correlated to transcriptional regulation and protein modification.

The global changes of alternative splicing in preimplantation

Previous studies have found that human major ZGA genes are particularly in connection with RNA splicing, suggesting that AS may play a crucial part in the development of preimplantation embryo. For the specific number of differentially AS events (DASEs) identified between each successional stage of human (Table 3) and the proportion of five types in each stage (Figure 2A), the results showed that SE events were the most common in all stages, followed by MXE, 63.6% and 18.6% of all AS events, respectively. The maximum DASEs occurred from 8-cell to morula, followed by 4-cell to 8-cell stage, and the largest number of stage-specific splicing events was also 8-cell to morula (Figure 2B). These pieces of evidence support our previous conclusion that the 8-cell stage is an essential stage during preimplantation development.

A similar splicing pattern was also observed in mice, the number of DASEs from 1-cell to 2-cell reached the peak (Figure S2A and Table S2). In addition, 267 splicing events occurred in 1-cell to 2-cell, which was the maximum number of stage-specific splicing events (Figure S2B).

Both in human and mouse data, only a few differentially spliced genes are differentially expressed genes at the same time (Figures 2C and S2C). We also found that the time change of splicing events tends to be consistent with that of transcript expression (Figures 1B, 2A, S1B, and S2A), which indicates that the distribution of AS is dynamic during preimplantation embryo development and these discoveries are in accordance with previous studies.[17,18]

Verification of differential alternative splicing

Mouse 2-cell and 4-cell embryo were collected for total RNA isolation, reverse transcription, and PCR detection. We found some exon-skipping events that are different between these two stages. Results of agarose gel separation experiment showed that if a gene has two bands, it means that the gene has detected two different isoforms. We chose Gapdh as a reference gene. Smc4 (ENSMUSG00000034349) and Sycp3 (ENSMUSG00000020059.5) were alternatively spliced at different exon-skipping level. Although no significant isoform difference was detected between Bag6 and Pkmyt1, the gene expression levels of Bag6 and Pkmyt1 were not consistent in the two stages (Figure 2D).

Maternal and ZGA genes that undergo splicing are translational activated

We examined how many genes in the maternal and ZGA genes were spliced themselves. The results showed that only a small number of these three types of genes were differentially spliced in both human and mouse data. Among them, human maternal RNA accounted for the highest proportion, 10.44% (40 of 383), followed by mouse maternal RNA, 10.27% (99 of 964) of genes were differentially spliced. Although human major ZGA contains the most genes, only 9.25% (160 of 1730) of genes were differential splicing genes. Meanwhile, only 4.06% (19 of 468) of mouse major ZGA genes were differential splicing genes, which was the lowest percentage (Figure 2E). This means that the splicing events itself may not play a particularly important roles in the development of early embryos as we thought. Hence, we checked the translational efficiency of the differentially spliced genes in these three types of genes. Almost all of the genes were in a state of translational activation ($\log_2$(TE+1) > 0).

Table 2. The number of transcripts during the six developmental stage in mouse

	oocyte	1-cell	2-cell	4-cell	8-cell	morula
0<FPKM≤1	6244	7338	6116	5414	5390	7085
1<FPKM≤10	4590	5458	5677	5354	4288	4823
10<FPKM≤100	3038	3673	3622	3527	3150	3528
FPKM>100	906	704	449	657	639	910
Sum	14778	17173	15864	14952	13467	/

Table 3. The number of DASEs in human

Stage	SE	RI	MXE	A5SS	A3SS	Sum
OC->1C	270	15	138	21	26	470
1C->2C	214	18	54	17	42	345
2C->4C	54	8	14	5	23	104
4C->8C	441	31	92	41	52	657
8C- > MC	1409	109	401	144	115	2178
Sum	2388	181	699	228	258	/

DASEs Cutoff: $p < 0.05$, FDR<0.05 and $|\Delta PSI|>0.1$.

Moreover, the dynamic changes of the translation activity of various genes were consistent with their biological processes, such as the translation efficiency of the spliced genes in mouse major ZGA reached the peak at the 2-cell stage (Figures 2F and S2D). The above findings suggest that although splicing events may not occupy a major position in early embryonic development, they still play an important role.

Splicing genes in major ZGA are specifically associated with cell cycle and metabolic processes

We used to consider the differentially expressed genes were the genes that played a crucial part in the activity of a living organism. However, our studies have found that those genes whose overall expression level have not changed but whose splicing patterns have changed may also play an import role.

To further study the function of DASE in human 8-cell to morula, we utilized the Metascape to analyze the given gene list. For each gene list, pathway and process enrichment analysis has been carried out with GO Biological Processes and Reactome Gene Sets. We presented the top 20 clusters with their representative enriched terms and these terms were rendered as a network plot. As Figure 3A shows, 11.1% of genes were clustered in Metabolism of RNA (R-HAS-8953854) and 10.16% were obtained in Cell Cycle (R-HAS-1640170). We also observed the blastocyst development (GO:0001824), mRNA metabolic process (GO:0016071) and Cell cycle (mmu04110) in the enrichment analysis results of mice 1-cell to 2-cell DASEs (Figure 3B). These suggest that AS genes widely affect basic biological progress, which may be a preparation for subsequent cell proliferation and differentiation.

Identification of RBP regulators

In order to identify the molecular participants associated with DASEs during preimplantation, we referred to the pipeline of Li et al. and designed a workflow to identify RBP regulators (Figure 4A). We assumed that the expression level of the target RBPs were related to the IncLevel of the splicing event, and the RBP regulators were screened by the Spearman correlation coefficient.

A total of 1,961 RBP genes were collected in human (95% are protein-coding), and 1,868 genes in mice were obtained after human-mouse homologous gene conversion. Human RBP genes involved a total of 1,764 genes that corresponded one-to-one with mouse RBP genes, while 52 human RBP genes corresponded to multiple mouse homologous RBP genes and 197 genes for which no homologous gene could be found in mice (Figure 4B).

In general, among the six stages of early embryo development, we predicted 242 and 22 RBP regulators in human and mouse respectively, the final prediction results can be seen in Data S1 and Table S3. We compared the relationship between predicted RBP regulators and DASEs (Figure 4C), 3.3% and 0.2% of RBPs occurred isoform switch events, suggesting the possibility that these RBPs may not only do they important function as gene regulators, but their different transcripts may also have various genetic functions. 2.9% (7 of 242) of RBPs are the members of eukaryotic initiation factor (EIF3J, EIF3D, EIF4G1, EIF3B, EIF3G, EIF4A3, EIF5A2), implying that different isoforms of the factors may play a different role in the eukaryotic initiation of the translation process. The predicted regulators were displayed according to classification and correlation. The height of the columns represented the absolute value of correlation coefficient, and the sequence of genes from left to right was arranged according to expression value (Figures 4D and 4E). In human data, 23 RBP regulators were predicted to be associated with both splicing active (SA) events and splicing repressive (SR) events, such as PFEN1, RBM24, and EIF3D (Figure 4D). In mouse data, only three RBPs were predicted to be associated with SA and SR, including Mak16, Utp23, and Zgpat (Figure 4E).

We checked the RBPs that was most frequently positively or negatively correlated with DASEs. Interestingly, previous research found that eukaryotic initiation factor 3 subunit D (EIF3D) knockdown influences the progress of preeclampsia through activating the phosphorylation of ERK1/2 and MEK1.[22] Although the expression level of RNA-binding motif protein 24 (RBM24) through all preimplantation stage is relatively low (Figure S3), it can serve as a key splicing regulator to control the spectrum development.[23,24] Meanwhile, differentially spliced RBP regulators Hars2 (Figure 4C) that predicted in mice is first reported to have a mutation that causes perrault syndrome, which is composed of symptoms of premature ovarian failure and hearing loss.[25,26] All these observations suggest that a comprehensive analysis of DASEs can potentially capture RBP related to reproductive development in early embryos. In addition, to verify the reliability of the pipeline, we tended to combine the predicted results with the RBP motifs for analysis.

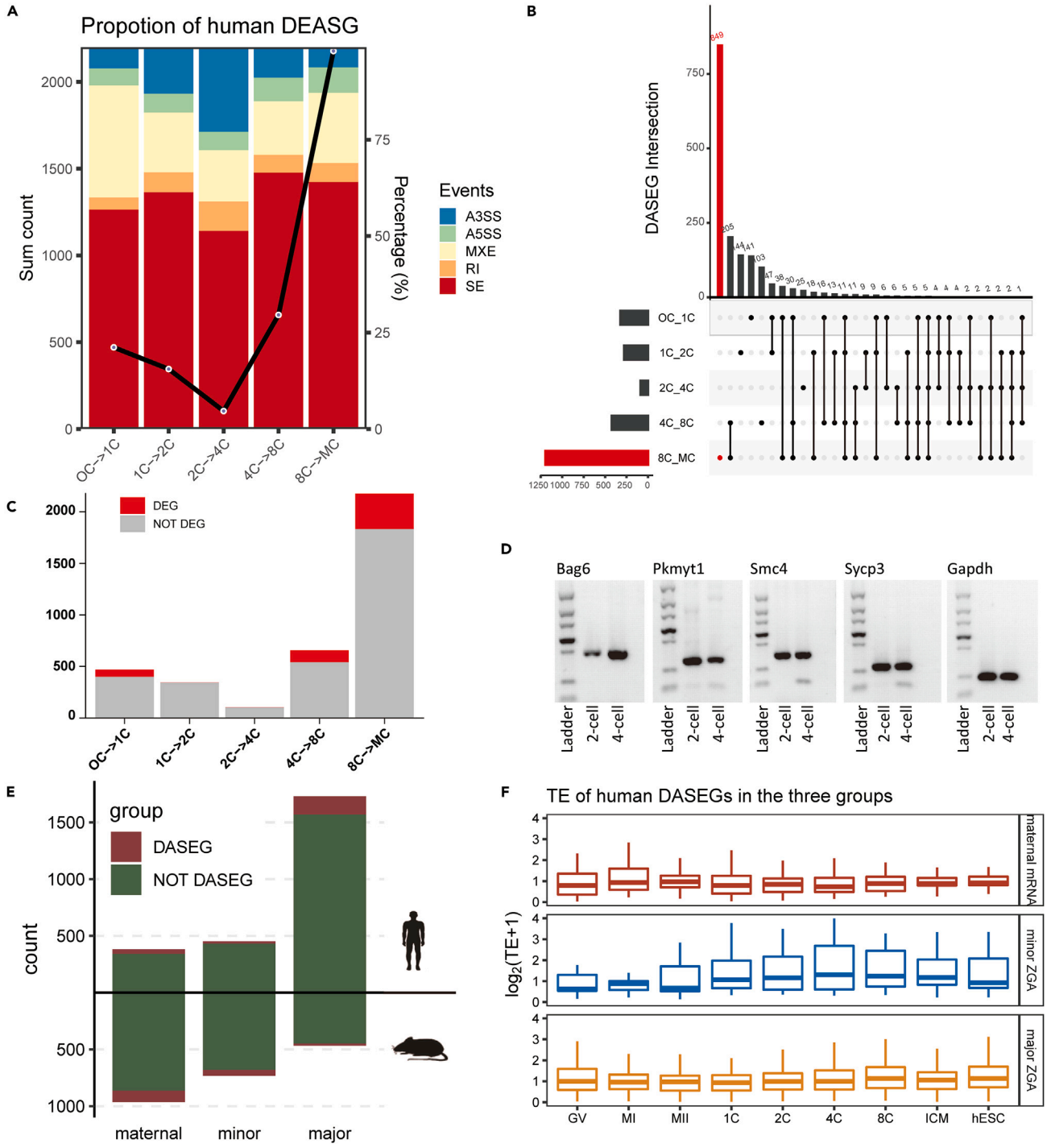

Figure 2. AS profiles during early embryonic development in human

(A) The statistic of human DASEs. The bar plot reveals the proportion of different modes of AS events and the line graph represents the number of all DASEs.

(B) Upset plot exhibits the relationship of genes which happened alternative splicing through all stages.

(C) The relationship between alternatively spliced genes and differentially expressed genes.

(D) The different isoforms of the gene were verified by agarose gel electrophoresis.

(E) The relationship between differential splicing genes and the three types of genes (maternal RNA, minor ZGA, and major ZGA).

(F) Translational efficiency of differential splicing genes in maternal RNA, major ZGA, and minor ZGA genes in human.

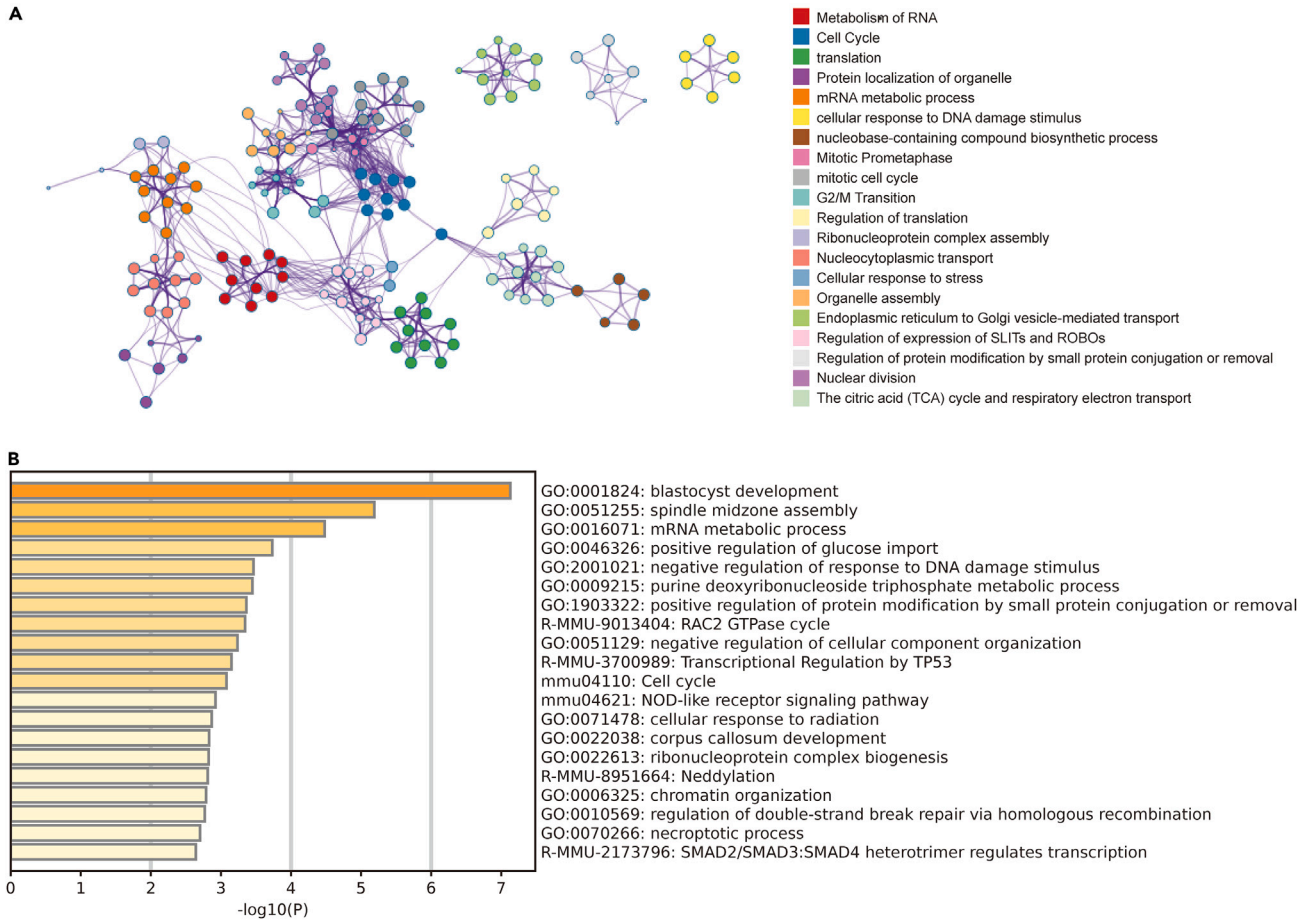

Figure 3. Functional enrichment of splicing genes in the major wave of ZGA

(A) Cluster the functional enrichment terms by Metascape and exhibit the top 20 clusters with their representative enriched entries in alternatively spliced genes without expression switch from human 8-cell to morula. Different clusters were filled with different colors.

(B) The bar plot of parent enriched entries from mouse 1-cell to 2-cell.

HNRNPK and SRSF2 are key factors during human zygotic genome activation

Next, we utilized rMAPS to identify the RBP binding sites which have position-dependent functions via the results of rMATS from human 8-cell to morula. Take the intersection of the rMAPS results and predicted RBP regulators, a list of 14 RBPs were obtained, of these RBPs, we found HNRNPK (Heterogeneous nuclear ribonucleoprotein K) and SRSF2 (Serine and arginine rich splicing factor 2) are overexpressed in 8-cell stage (Figure 5A), and they have RNA binding sites (motifs) that are enriched in the 5′ or 3′ introns of the cassette exons that are different expressed between 8-cell and morula stage (Figure 5B). A more interesting thing is that when we check the correlated DASEs with HNRNPK and SRSF2, the isoform switch events were happened both in MCRS1 (Microspherule protein 1) and TIA1 (T-cell-restricted intracellular antigen 1). Based on previous research MCRS1 is essential during early murine development, we can observe that the significant different isoform usage happened in ENST00000546244 and ENST00000548602 is an alternative 3′ splicing site event. Likewise, TIA1 was discovered changing use of nonsense-mediated mRNA decay (NMD) sensitive isoform (Figure 5C). These hint that HNRNPK and SRSF2 are key RNA splicing regulators during embryogenesis and the possible mechanism is via regulating MCRS1 and TIA1.

Since the amino acid sequences of HNRNPK and SRSF2 are highly conserved between human and mouse, we microinjected effective siRNA-Hnrnpk and siRNA-Srsf2 (Figures S4A and S4B) in mouse zygotes to observe their separate functions. Interestingly, a slight development delay was observed at D4 (morula stage, $p = 0.037$, 13.72 ± 4.44), with a more significant delay at D5 (blastocyst stage, $p = 0.002$, 40.41 ± 5.24) over time (Figures 5D and 5E) in siRNA-Srsf2 group. However, when observing of siRNA-Hnrnpk group, no significant difference in development rate was observed at any stage (Figures S5A and S5B).

Eif4a3, Mak16, Utp23 regulate mouse preimplantation development

We then investigated the mouse RBP candidate regulators whose function were little known in the reproductive system. The siRNA against target gene or negative controls were injected into 1-cell embryos in parallel (Figure 6A). Each siRNA can knockdown (KD) the expression of

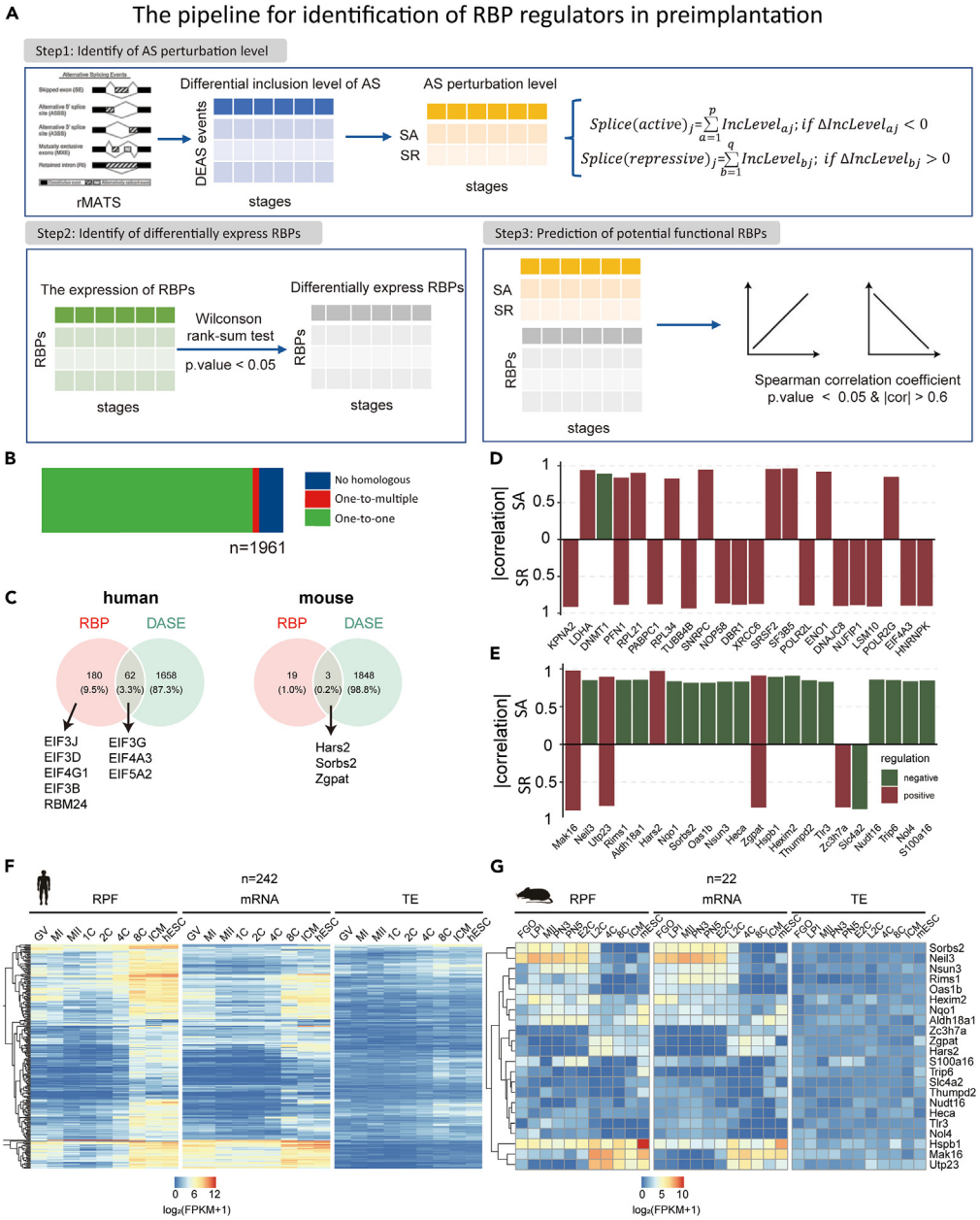

Figure 4. Identifying RBP regulators of AS in preimplantation

(A) The workflow for identifying RBP regulators.

(B) Homologous gene conversion from human to mouse.

(C) The relationship between predicted RBP regulators and DASEs.

(D and E) The exhibition of predicted RBP regulators according to correlation and splicing activity classification. The height of the column represents the absolute value of the correlation coefficient and the order from left to right is arranged according to the expression value. D for human and E for mouse.

(F and G) Translation efficiency of predicted RBPs, F for human and G for mouse.

target genes in neuro-2a cell line (Figures S4C, S4D, and S4E). Although the difference on D4 (morula stage) was not statistically significant, the development was slightly delayed for Eif4a3 KD embryos, which became significant ($p = 0.012$, 36.25 ± 10.19) on D5 (blastocyst stage) (Figures 6B, 6C, and 6D). In Mak16 KD embryos, development rate of D3 (4-cell stage) and D5 both showed statistical differences, while the rate of D4 did not (Figure 6E). However, the proportion of cells at each stage during these three days showed a slight developmental delay (Figure 6F). Development did not show a statistical difference until D5 ($p = 0.041$, 22.49 ± 7.59) in Utp23 KD embryos (Figure 6G). We further observed that there was no developmental delay on D4, but a slight delay on D5 (Figure 6H).

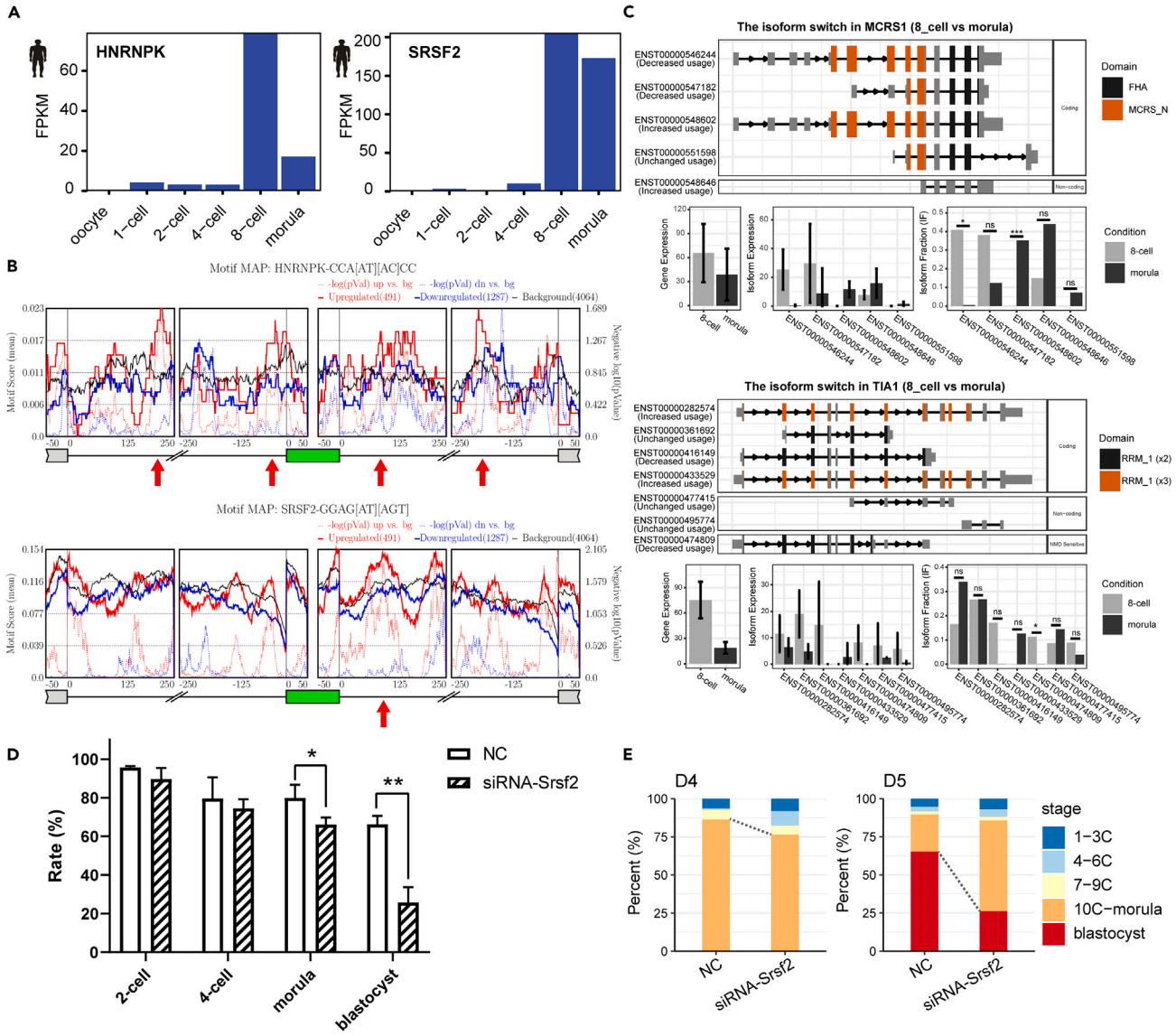

Figure 5. Expression level of predicted RBP regulators and RNA binding motif enrichment analysis reveals the target isoform of the combination

(A) The transcriptome expression level of HNRNPK and SRSF2 across all stages.

(B) The RNA binding sites (motifs) of HNRNPK and SRSF2.

(C) The condition of isoform switch events of MCRS1 and TIA1.

(D) The statistical chart of embryo development rate at each stage between NC group (N = 95) and siRNA-Srsf2 group (N = 84). There were significant differences in morula rate ($p = 0.037$, 13.72 ± 4.44) and blastocyst rate ($p = 0.002$, 40.41 ± 5.24). Data are represented as mean ± SEM.

(E) Embryo phenotypes of Srsf2 KD on day 4 (D4, morula stage) and day 5 (D5, blastocyst stage) after injection across 3 batches.

Eif4a3 is involved in mouse preimplantation RNA processing

We next investigated the regulatory role of Eif4a3 and global RNA changes due to Eif4a3 knockdown in mouse embryos. Embryonic transcriptomes were compared between NC and siRNA-Eif4a3 groups 96 h post-microinjection using high-throughput sequencing (Smart-seq2). Three biological replicates were collected for each group, and the data is deposited in GEO: GSE247316. In our transcriptome data, we examined the expression of Eif4a3 and found that it significantly decreased in the siRNA-Eif4a3 group, as shown in Figure 7A ($p = 0.045$). We also discovered that Eif4a3 knockdown affected a total of 5445 DASEs (FDR <0.05 and $|\Delta \text{IncLevel}| > 0.1$). The majority of the DASEs were skipped exon (3622), while others were alternative 5′ splice site (323), alternative 3′ splice site (358), mutually exclusive exons (764), and retained intron (378) (Figure 7B). These DASEs occurred in a total of 2565 genes and were clustered by mfuzz according to the

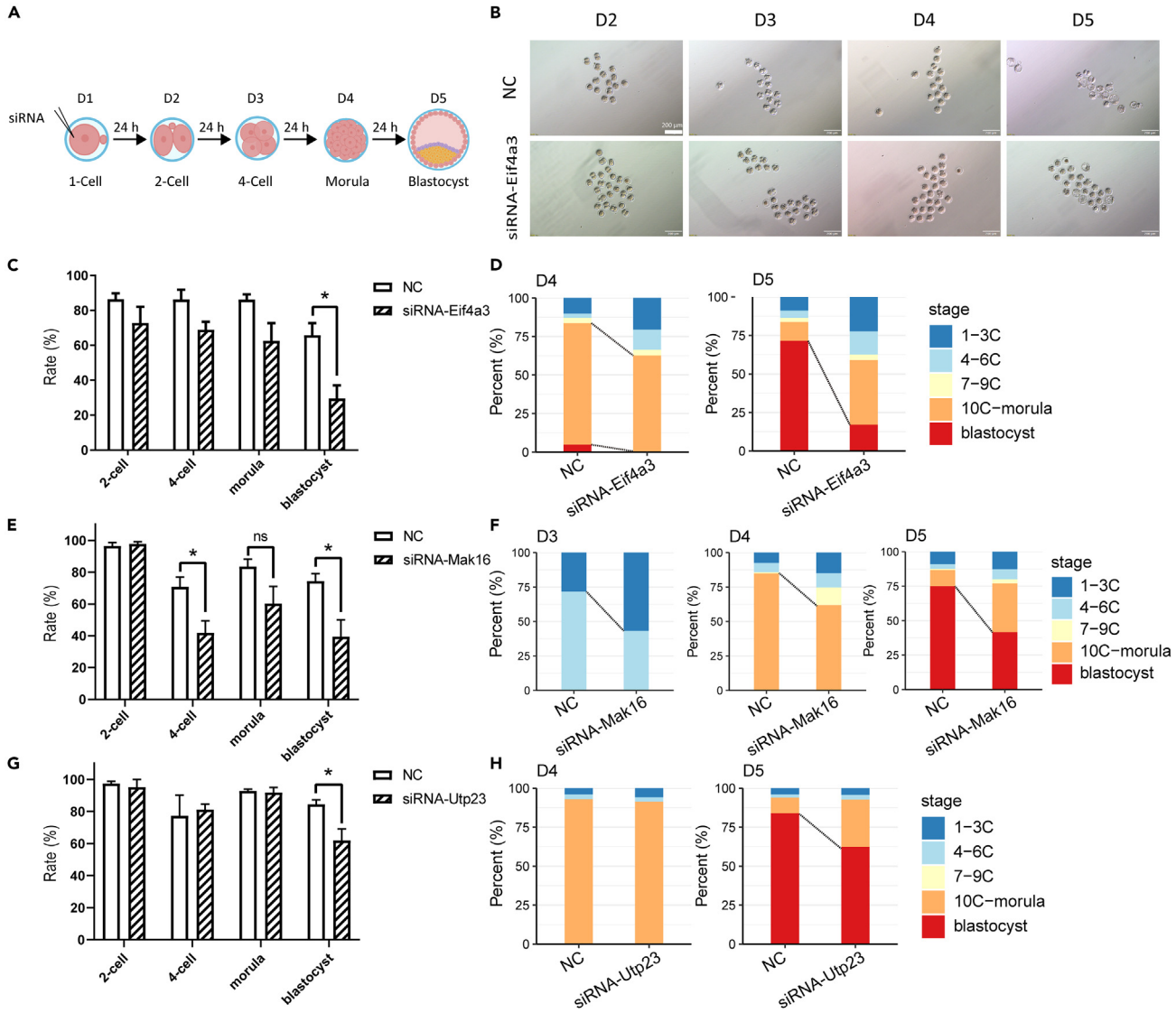

Figure 6. Eif4a3, Mak16, Utp23 knockdown embryos showed defects in early development

(A) Schematic of gene knockdown experiments. Zygotes were injected with either siRNA-targeted-gene or control siRNA, and the embryos were observed every 24 h until the blastocyst stage was reached 96 h later.

(B) Morphologies of Eif4a3 KD and control embryos, scale bar for 20 μm.

(C) The statistical chart of embryo development rate at each stage between NC group (N = 70) and siRNA-Eif4a3 group (N = 40). There was a significant difference in blastocyst rate ($p = 0.012$, 36.25 ± 10.19). Data are represented as mean ± SEM.

(D) Embryo phenotypes of Eif4a3 KD on day 4 and day 5 after injection across 3 batches.

(E) The statistical chart of embryo development rate at each stage between NC group (N = 85) and siRNA-Mak16 group (N = 101). There were significant differences in 4-cell rate ($p = 0.024$, 29.05 ± 9.63) and blastocyst rate ($p = 0.023$, 34.90 ± 11.55).

(F) Embryo phenotypes of Mak16 KD on day 3, day 4, and day 5 after injection across 3 batches.

(G) The statistical chart of embryo development rate at each stage between NC group (N = 118) and siRNA-Utp23 group (N = 69). There were significant differences in blastocyst rate ($p = 0.041$, 22.49 ± 7.59).

(H) Embryo phenotypes of Utp23 KD on day 4, and day 5 after injection across 3 batches.

transcriptome expression. We then subjected each cluster to Gene Ontology (GO) analysis and found that each was enriched with a number of terms related to RNA processing, such as RNA splicing, mRNA processing, and ncRNA metabolic process.

Moreover, we observed several key genes related to embryonic development in the differentially AS genes, such as Ybx1, Sycp3, and Sirt2,[27–31] indicating that the knockdown of Eif4a3 could affect the global splicing state during embryo development and, as a result, hinder the development of embryos.

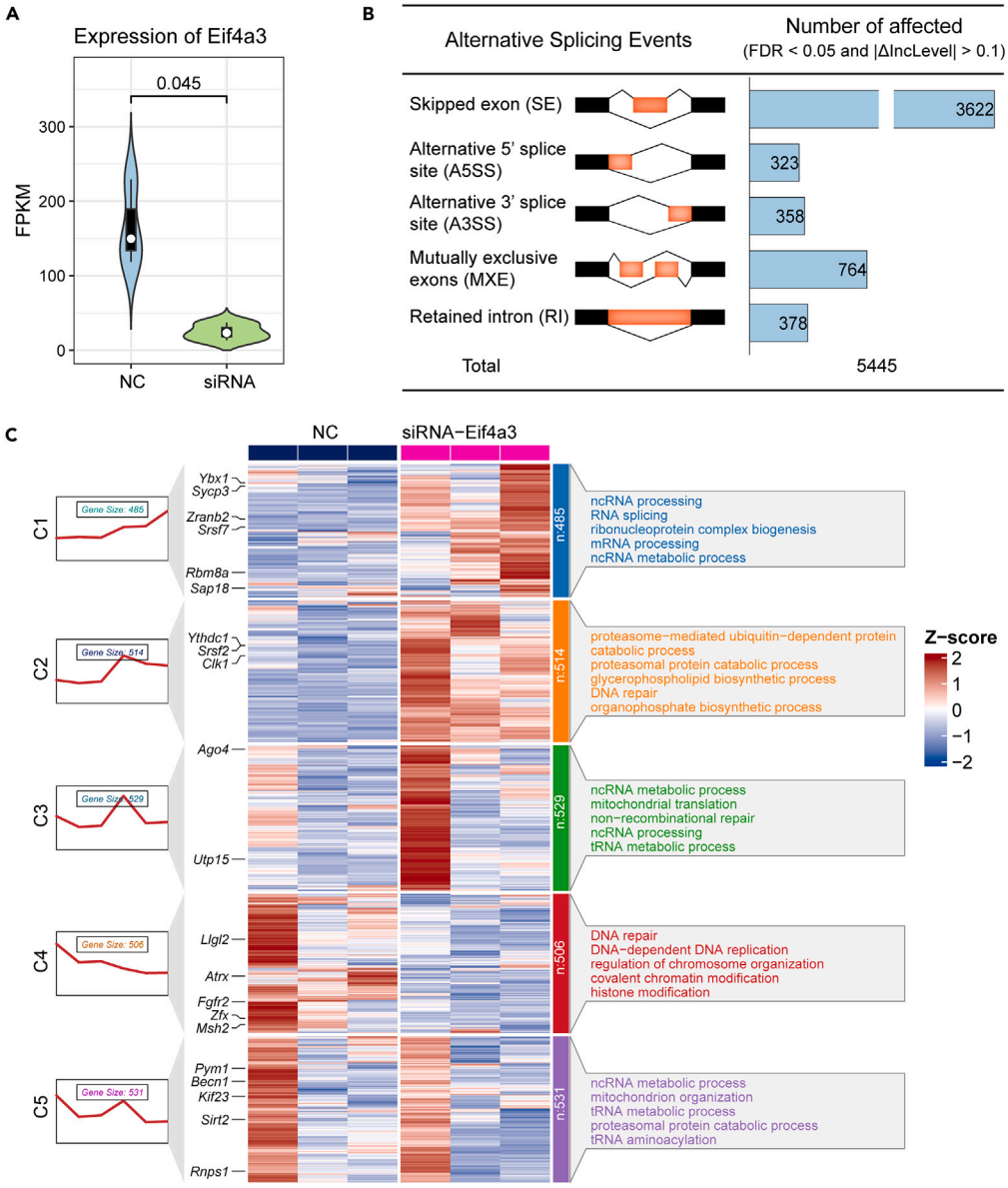

Figure 7. Alternative splicing perturbation in Eif4a3 KD mouse embryos

(A) The FPKM value of Eif4a3 in transcriptome sequencing.

(B) The number of all kinds of differentially alternative splicing events.

(C) Expression heatmap and Gene Ontology annotation of all genes which involved in differentially alternative splicing events. C1 to C5 refer to different gene clusters which clustered by mfuzz method according to the transcriptome expression level. The line plot exhibits the expression changes of each cluster in samples. In the middle of the plot is the heatmap of gene expression transformed by *Z* score. The text on the right is the biological function annotation of the corresponding cluster genes.

DISCUSSION

We combined multiple datasets to summarize the AS events landscape of human and mouse preimplantation development at the transcriptome and translatome levels. Previous studies have shown that AS is dynamic during preimplantation development in mouse.[17,18] Our study confirms this observation not only in mouse, but also in human. It is worth nothing that both human and mouse are the most observed splicing events during ZGA, which may also be due to the fact that ZGA takes a long period and requires more complex regulation. Unlike mouse, human major ZGA genes are more involved in the metabolic process of RNA splicing regulation, which indicates that the biological process and function of human major ZGA are more delicate and complex than mouse. Besides, wo also found that although only a small proportion of maternal RNA and ZGA genes are differentially spliced genes, the spliced genes are translation

activated and only a small part of them are differentially expressed genes in early embryos. This shows the importance of splicing in the regulation of early embryos. However, finding truly functional differential splicing evens is very difficult, hence we turn to look for these upstream RBP regulators.

The latest research system shows AS events pattern of humans, mice and cows but does not focus on the RBP regulators that regulate splicing.[16] More and more evidence shows that RBPs can regulate the expression of transcripts and are reported to be related to reproductive development.[20,32–34] In this study, we integrated differential splicing events and genome-wide expression between human and mouse, and processed a computational method to identify splicing-related RBPs in early embryos. In human, 242 RBPs related to the occurrence of AS events were predicted. Through expression screening and manual literature research, we found that HNRNPK and SRSF2 are two valuable RBP regulators in human. Since it is challenging to obtain human samples for verification experiments, we decided to investigate the functional roles of SRSF2 and HNRNPK in mouse zygotes by microinjecting siRNA of homologous genes. Both SRSF2 and HNRNPK are highly conserved in the protein sequences of human and mouse. Our findings show that the siRNA-Srsf2 group significantly reduced the development rate during the morula and blastocyst stage. However, no change was observed in the siRNA-Hnrnpk group. In addition, we also identified their binding motifs in rMAPS. They work by combining with downstream introns at the 3′ end or upstream introns at the 5′ end. In our prediction, the splicing events of MCRS1 and TIA1 were correlated with both of HNRNPK and SRSF2. Through isoform switch analysis, it was found that A3SS was occurred between the two isoforms of MCRS1. Although, the role of A3SS during early embryonic development, 3′-UTR isoform switch is common during mouse oocyte maturation.[35] What is even more interesting is that the transcript with significant changes in TIA1 is NMD-sensitive transcripts. As an important RNA monitoring mechanism in eukaryotic cells, NMD can identify and explain the mRNA with early termination codon in the open reading frame.[36] It has been proved that TIA takes a crucial part in embryonic development,[37] which suggests that TIA may play a role through NMD-related mechanisms.

At the same time, we also investigated the function of mouse predicted RBPs by microinjecting targeted siRNA into mouse zygotes. The knockdowns of Eif4a3, Mak16 and Utp23 all delayed embryonic development, indicating the reliability of predicting RBP regulators in early embryonic development by splicing level. We also conducted Smart-seq2 on Eif4a3-knockdown embryos to examine the overall alterations in their splicing landscape. Our analysis revealed a total of 5445 DASEs in 2565 genes, which were found to be associated with embryonic development, RNA metabolism, and DNA repair. As an important component of exon junction complex (EJC), EIF4A3 is a nucleation center that recruits other components to form EJCs. Binding of EJCs to different cofactors can mediate the progression of different factor specificities, and the functional role of EJCs has been identified as key to the normal progression of embryonic and neural development.[38–41] We speculated that knockdown of Eif4a3 in embryos would lead to EJC assembly failure, affecting the splicing and fate of multiple genes and thus resulting in developmental delay. Mak16 and Utp23 have only a few sporadic case reports,[42–45] and their functions and mechanism are unclear. Due do the limitation of experimental materials and time, we did not further study their molecular mechanism, which needs further research.

Overall, the dynamic maps of DEGs and DASEs during preimplantation development were established and analyzed comprehensively. It is speculated that RBPs can play a role in early embryonic development through its own AS and regulation of other genes to produce different isoforms. 242 human and 22 mouse RBP regulators that may play an important role in embryogenesis were predicted. This study provides a guide or suggestion for further experimental verification to clarify the regulatory mechanism of preimplantation development.

Limitations of the study

Indeed, our research has other limitations. First, our sample size is too small to control the uniformity of sample quality. Second, with the change of upstream technology of gene sequencing, the third-generation sequencing technology of ultralong reading is also booming, and the most representative ones are Pacific Bioscience (PacBio) and Oxford Nanopore Technologies (ONT). Take PacBio as an example; its Isoform-sequencing (Iso-seq) uses long-read sequence to sequence transcript isoforms up to 10 kb,[46] and the analysis results of A3SS and A5SS splicing types would be more accurate than short-read sequencing.[35,47] However, due to technical limitations, the third-generation sequencing technology has not been developed to the resolution of a single cell within the scope of commerce, otherwise the recognition and analysis of splice changes might be more accurate.

STAR★METHODS

Detailed methods are provided in the online version of this paper and include the following:

- KEY RESOURCES TABLE
- RESOURCE AVAILABILITY
  - Lead contact
  - Materials availability
  - Data and code availability
- EXPERIMENTAL MODEL AND STUDY PARTICIPANT
  - Mice and ethics
  - Culture and collection of mouse embryos
  - Gene knockdown by siRNA microinjection
- METHOD DETAILS

- Transcriptome data analysis
- R2-lite data analysis
- Temporal dynamic clustering analysis of gene expression profiles
- Differential alternative splicing events identification
- Identification of isoform switch events
- Validation of differential alternative splicing events
- Function enrichment analysis
- Prediction of DASEs-related RBP regulators
- Smart-seq2 for Eif4a3-knockdown embryos

● QUANTIFICATION AND STATISTICAL ANALYSIS

SUPPLEMENTAL INFORMATION

Supplemental information can be found online at https://doi.org/10.1016/j.isci.2024.109104.

ACKNOWLEDGMENTS

This research was financially supported by grants from National Natural Science Foundation of China (81971451, 31900605), Innovative and Entrepreneurial Team of Jiangsu Province (JSSCTD202144) and Innovative and Entrepreneurial Talent Program of Jiangsu Province.

We appreciate the selfless and professional advice by Xinuo Li and Qiulun Lu from China Pharmaceutical University, and Shan Lu in School of Pharmacy, Nanjing Medical University.

AUTHOR CONTRIBUTIONS

J.C. and Y.H. contributed equally to this study. J.C. collected the datasets and analyzed the omics data. Y.H. did the embryo-related experiments. T.W. and G.Y. conducted the microinjection experiment, L.C., H.L., S.H., S.Y., H.M. and N.L. helped collecting fallopian tubes. Y.Q., C.M. and R.F. designed the study. J.C., C.M. and R.F. wrote and revised the manuscript. All authors reviewed and approved. All authors contributed to the article and approved the submitted version.

DECLARATION OF INTERESTS

The authors declare that they have no conflict of interest.

Received: January 19, 2023
Revised: November 16, 2023
Accepted: January 30, 2024
Published: February 2, 2024

REFERENCES

1. Zou, Z., Zhang, C., Wang, Q., Hou, Z., Xiong, Z., Kong, F., Wang, Q., Song, J., Liu, B., Liu, B., et al. (2022). Translatome and transcriptome co-profiling reveals a role of TPRXs in human zygotic genome activation. Science *378*, eabo7923. https://doi.org/10.1126/science.abo7923.
2. Gao, Y., Liu, X., Tang, B., Li, C., Kou, Z., Li, L., Liu, W., Wu, Y., Kou, X., Li, J., et al. (2017). Protein Expression Landscape of Mouse Embryos during Pre-implantation Development. Cell Rep. *21*, 3957–3969. https://doi.org/10.1016/j.celrep.2017.11.111.
3. Sha, Q.-Q., Zhang, J., and Fan, H.-Y. (2019). A story of birth and death: mRNA translation and clearance at the onset of maternal-to-zygotic transition in mammals. Biol. Reprod. *101*, 579–590. https://doi.org/10.1093/biolre/ioz012.
4. Sha, Q.-Q., Zheng, W., Wu, Y.-W., Li, S., Guo, L., Zhang, S., Lin, G., Ou, X.-H., and Fan, H.-Y. (2020). Dynamics and clinical relevance of maternal mRNA clearance during the oocyte-to-embryo transition in humans. Nat. Commun. *11*, 4917. https://doi.org/10.1038/s41467-020-18680-6.
5. Sha, Q.-Q., Zhu, Y.-Z., Li, S., Jiang, Y., Chen, L., Sun, X.-H., Shen, L., Ou, X.-H., and Fan, H.-Y. (2020). Characterization of zygotic genome activation-dependent maternal mRNA clearance in mouse. Nucleic Acids Res. *48*, 879–894. https://doi.org/10.1093/nar/gkz1111.
6. Yu, C., Ji, S.-Y., Sha, Q.-Q., Dang, Y., Zhou, J.-J., Zhang, Y.-L., Liu, Y., Wang, Z.-W., Hu, B., Sun, Q.-Y., et al. (2016). BTG4 is a meiotic cell cycle-coupled maternal-zygotic-transition licensing factor in oocytes. Nat. Struct. Mol. Biol. *23*, 387–394. https://doi.org/10.1038/nsmb.3204.
7. Sha, Q.-Q., Yu, J.-L., Guo, J.-X., Dai, X.-X., Jiang, J.-C., Zhang, Y.-L., Yu, C., Ji, S.-Y., Jiang, Y., Zhang, S.-Y., et al. (2018). CNOT6L couples the selective degradation of maternal transcripts to meiotic cell cycle progression in mouse oocyte. EMBO J. *37*, e99333. https://doi.org/10.15252/embj.201899333.
8. Lee, M.T., Bonneau, A.R., and Giraldez, A.J. (2014). Zygotic genome activation during the maternal-to-zygotic transition. Annu. Rev. Cell Dev. Biol. *30*, 581–613. https://doi.org/10.1146/annurev-cellbio-100913-013027.
9. Jukam, D., Shariati, S.A.M., and Skotheim, J.M. (2017). Zygotic Genome Activation in Vertebrates. Dev. Cell *42*, 316–332. https://doi.org/10.1016/j.devcel.2017.07.026.
10. Asami, M., Lam, B.Y.H., Ma, M.K., Rainbow, K., Braun, S., VerMilyea, M.D., Yeo, G.S.H., and Perry, A.C.F. (2022). Human embryonic genome activation initiates at the one-cell stage. Cell Stem Cell *29*, 209–216.e4. https://doi.org/10.1016/j.stem.2021.11.012.
11. Latham, K.E., and Schultz, R.M. (2001). Embryonic genome activation. Front. Biosci. *6*, D748–D759. https://doi.org/10.2741/latham.
12. Vassena, R., Boué, S., González-Roca, E., Aran, B., Auer, H., Veiga, A., and Izpisua Belmonte, J.C. (2011). Waves of early transcriptional activation and pluripotency program initiation during human preimplantation development. Development *138*, 3699–3709. https://doi.org/10.1242/dev.064741.
13. Chen, M., Yang, W., Liu, N., Zhang, X., Dong, W., Lan, X., and Pan, C. (2019). Pig Hsd17b3: Alternative splice variants expression, insertion/deletion (indel) in promoter region and their associations with male reproductive

traits. J. Steroid Biochem. Mol. Biol. *195*, 105483. https://doi.org/10.1016/j.jsbmb.2019.105483.
14. Anamthathmakula, P., Kyathanahalli, C., Ingles, J., Hassan, S.S., Condon, J.C., and Jeyasuria, P. (2019). Estrogen receptor alpha isoform ERdelta7 in myometrium modulates uterine quiescence during pregnancy. EBioMedicine *39*, 520–530. https://doi.org/10.1016/j.ebiom.2018.11.038.
15. Li, J., Lu, M., Zhang, P., Hou, E., Li, T., Liu, X., Xu, X., Wang, Z., Fan, Y., Zhen, X., et al. (2020). Aberrant spliceosome expression and altered alternative splicing events correlate with maturation deficiency in human oocytes. Cell Cycle *19*, 2182–2194. https://doi.org/10.1080/15384101.2020.1799295.
16. Wyatt, C.D.R., Pernaute, B., Gohr, A., Miret-Cuesta, M., Goyeneche, L., Rovira, Q., Salzer, M.C., Boke, E., Bogdanovic, O., Bonnal, S., and Irimia, M. (2022). A developmentally programmed splicing failure contributes to DNA damage response attenuation during mammalian zygotic genome activation. Sci. Adv. *8*, eabn4935. https://doi.org/10.1126/sciadv.abn4935.
17. Tian, G.G., Li, J., and Wu, J. (2020). Alternative splicing signatures in preimplantation embryo development. Cell Biosci. *10*, 33. https://doi.org/10.1186/s13578-020-00399-y.
18. Xing, Y., Yang, W., Liu, G., Cui, X., Meng, H., Zhao, H., Zhao, X., Li, J., Liu, Z., Zhang, M.Q., and Cai, L. (2020). Dynamic Alternative Splicing During Mouse Preimplantation Embryo Development. Front. Bioeng. Biotechnol. *8*, 35. https://doi.org/10.3389/fbioe.2020.00035.
19. Cheng, R., Zheng, X., Wang, Y., Wang, M., Zhou, C., Liu, J., Zhang, Y., Quan, F., and Liu, X. (2020). Genome-wide analysis of alternative splicing differences between oocyte and zygote. Biol. Reprod. *102*, 999–1010. https://doi.org/10.1093/biolre/ioaa004.
20. Yu, L., Zhang, H., Guan, X., Qin, D., Zhou, J., and Wu, X. (2021). Loss of ESRP1 blocks mouse oocyte development and leads to female infertility. Development *148*, dev196931. https://doi.org/10.1242/dev.196931.
21. Schultz, R.M. (2002). The molecular foundations of the maternal to zygotic transition in the preimplantation embryo. Hum. Reprod. Update *8*, 323–331. https://doi.org/10.1093/humupd/8.4.323.
22. Li, X., Wang, Z., Liu, G., and Guo, J. (2021). EIF3D promotes the progression of preeclampsia by inhibiting of MAPK/ERK1/2 pathway. Reprod. Toxicol. *105*, 166–174. https://doi.org/10.1016/j.reprotox.2021.09.006.
23. Grifone, R., Shao, M., Saquet, A., and Shi, D.-L. (2020). RNA-Binding Protein Rbm24 as a Multifaceted Post-Transcriptional Regulator of Embryonic Lineage Differentiation and Cellular Homeostasis. Cells *9*, 1891. https://doi.org/10.3390/cells9081891.
24. Grifone, R., Saquet, A., Xu, Z., and Shi, D.-L. (2018). Expression patterns of Rbm24 in lens, nasal epithelium, and inner ear during mouse embryonic development. Dev. Dynam. *247*, 1160–1169. https://doi.org/10.1002/dvdy.24666.
25. Pierce, S.B., Chisholm, K.M., Lynch, E.D., Lee, M.K., Walsh, T., Opitz, J.M., Li, W., Klevit, R.E., and King, M.-C. (2011). Mutations in mitochondrial histidyl tRNA synthetase HARS2 cause ovarian dysgenesis and sensorineural hearing loss of Perrault syndrome. Proc. Natl. Acad. Sci. USA *108*, 6543–6548. https://doi.org/10.1073/pnas.1103471108.
26. Jenkinson, E.M., Rehman, A.U., Walsh, T., Clayton-Smith, J., Lee, K., Morell, R.J., Drummond, M.C., Khan, S.N., Naeem, M.A., Rauf, B., et al. (2013). Perrault syndrome is caused by recessive mutations in CLPP, encoding a mitochondrial ATP-dependent chambered protease. Am. J. Hum. Genet. *92*, 605–613. https://doi.org/10.1016/j.ajhg.2013.02.013.
27. Deng, M., Chen, B., Liu, Z., Wan, Y., Li, D., Yang, Y., and Wang, F. (2022). YBX1 mediates alternative splicing and maternal mRNA decay during pre-implantation development. Cell Biosci. *12*, 12. https://doi.org/10.1186/s13578-022-00743-4.
28. Blyth, U., Craciunas, L., Hudson, G., and Choudhary, M. (2021). Maternal germline factors associated with aneuploid pregnancy loss: a systematic review. Hum. Reprod. Update *27*, 866–884. https://doi.org/10.1093/humupd/dmab010.
29. Tatone, C., Di Emidio, G., Barbonetti, A., Carta, G., Luciano, A.M., Falone, S., and Amicarelli, F. (2018). Sirtuins in gamete biology and reproductive physiology: emerging roles and therapeutic potential in female and male infertility. Hum. Reprod. Update *24*, 267–289. https://doi.org/10.1093/humupd/dmy003.
30. Yuan, L., Liu, J.-G., Hoja, M.-R., Wilbertz, J., Nordqvist, K., and Höög, C. (2002). Female germ cell aneuploidy and embryo death in mice lacking the meiosis-specific protein SCP3. Science *296*, 1115–1118. https://doi.org/10.1126/science.1070594.
31. Bertoldo, M.J., Listijono, D.R., Ho, W.-H.J., Riepsamen, A.H., Goss, D.M., Richani, D., Jin, X.L., Mahbub, S., Campbell, J.M., Habibalahi, A., et al. (2020). NAD+ Repletion Rescues Female Fertility during Reproductive Aging. Cell Rep. *30*, 1670–1681.e7. https://doi.org/10.1016/j.celrep.2020.01.058.
32. Harvey, S.E., Xu, Y., Lin, X., Gao, X.D., Qiu, Y., Ahn, J., Xiao, X., and Cheng, C. Coregulation of Alternative Splicing by hnRNPM and ESRP1 during EMT. RNA 24(10):1326-1338.
33. Williamson, D.J., Banik-Maiti, S., DeGregori, J., and Ruley, H.E. (2000). hnRNP C is required for postimplantation mouse development but Is dispensable for cell viability. Mol. Cell Biol. *20*, 4094–4105. https://doi.org/10.1128/MCB.20.11.4094-4105.2000.
34. Zhao, L.-W., Zhu, Y.-Z., Wu, Y.-W., Pi, S.-B., Shen, L., and Fan, H.-Y. (2022). Nuclear poly(A) binding protein 1 (PABPN1) mediates zygotic genome activation-dependent maternal mRNA clearance during mouse early embryonic development. Nucleic Acids Res. *50*, 458–472. https://doi.org/10.1093/nar/gkab1213.
35. He, Y., Chen, Q., Zhang, J., Yu, J., Xia, M., and Wang, X. (2021). Pervasive 3′-UTR Isoform Switches During Mouse Oocyte Maturation. Front. Mol. Biosci. *8*, 727614. https://doi.org/10.3389/fmolb.2021.727614.
36. Mailliot, J., Vivoli-Vega, M., and Schaffitzel, C. (2022). No-nonsense: insights into the functional interplay of nonsense-mediated mRNA decay factors. Biochem. J. *479*, 973–993. https://doi.org/10.1042/BCJ20210556.
37. Sánchez-Jiménez, C., and Izquierdo, J.M. (2013). T-cell intracellular antigen (TIA)-proteins deficiency in murine embryonic fibroblasts alters cell cycle progression and induces autophagy. PLoS One *8*, e75127. https://doi.org/10.1371/journal.pone.0075127.
38. Asthana, S., Martin, H., Rupkey, J., Patel, S., Yoon, J., Keegan, A., and Mao, Y. (2022). The Physiological Roles of the Exon Junction Complex in Development and Diseases. Cells *11*, 1192. https://doi.org/10.3390/cells11071192.
39. Xue, C., Gu, X., Li, G., Bao, Z., and Li, L. (2021). Expression and Functional Roles of Eukaryotic Initiation Factor 4A Family Proteins in Human Cancers. Front. Cell Dev. Biol. *9*, 711965. https://doi.org/10.3389/fcell.2021.711965.
40. Mao, H., McMahon, J.J., Tsai, Y.-H., Wang, Z., and Silver, D.L. (2016). Haploinsufficiency for Core Exon Junction Complex Components Disrupts Embryonic Neurogenesis and Causes p53-Mediated Microcephaly. PLoS Genet. *12*, e1006282. https://doi.org/10.1371/journal.pgen.1006282.
41. Kanellis, D.C., Espinoza, J.A., Zisi, A., Sakkas, E., Bartkova, J., Katsori, A.-M., Boström, J., Dyrskjøt, L., Broholm, H., Altun, M., et al. (2021). The exon-junction complex helicase eIF4A3 controls cell fate via coordinated regulation of ribosome biogenesis and translational output. Sci. Adv. *7*, eabf7561. https://doi.org/10.1126/sciadv.abf7561.
42. Ling, H.-Z., Xu, S.-Z., Leng, R.-X., Wu, J., Pan, H.-F., Fan, Y.-G., Wang, B., Xia, Y.-R., Huang, Q., Shuai, Z.-W., and Ye, D.Q. (2020). Discovery of new serum biomarker panels for systemic lupus erythematosus diagnosis. Rheumatology *59*, 1416–1425. https://doi.org/10.1093/rheumatology/kez634.
43. Crisóstomo-Vázquez, M.d.P., Marevelez-Acosta, V.A., Flores-Luna, A., and Jiménez-Cardoso, E. (2014). The MAK16 gene of Entamoeba histolytica and its identification in isolates from patients. Kor. J. Parasitol. *52*, 429–433. https://doi.org/10.3347/kjp.2014.52.4.429.
44. Fu, Z., Wang, C., Chen, Y., Zhang, X., Wang, X., and Xie, X. (2019). Down-regulation of UTP23 promotes paclitaxel resistance and predicts poorer prognosis in ovarian cancer. Pathol. Res. Pract. *215*, 152625. https://doi.org/10.1016/j.prp.2019.152625.
45. Vos, T.J., and Kothe, U. (2022). Synergistic interaction network between the snR30 RNP, Utp23, and ribosomal RNA during ribosome synthesis. RNA Biol. *19*, 764–773. https://doi.org/10.1080/15476286.2022.2078092.
46. Shah, A., Mittleman, B.E., Gilad, Y., and Li, Y.I. (2021). Benchmarking sequencing methods and tools that facilitate the study of alternative polyadenylation. Genome Biol. *22*, 291. https://doi.org/10.1186/s13059-021-02502-z.
47. Hu, Y., Shu, X.-S., Yu, J., Sun, M.-A., Chen, Z., Liu, X., Fang, Q., Zhang, W., Hui, X., Ying, Y., et al. (2020). Improving the diversity of captured full-length isoforms using a normalized single-molecule RNA-sequencing method. Commun. Biol. *3*, 403. https://doi.org/10.1038/s42003-020-01125-7.
48. Xue, Z., Huang, K., Cai, C., Cai, L., Jiang, C.y., Feng, Y., Liu, Z., Zeng, Q., Cheng, L., Sun, Y.E., et al. (2013). Genetic programs in human and mouse early embryos revealed by single-cell RNA sequencing. Nature *500*, 593–597. https://doi.org/10.1038/nature12364.
49. Xiong, Z., Xu, K., Lin, Z., Kong, F., Wang, Q., Quan, Y., Sha, Q.Q., Li, F., Zou, Z., Liu, L., et al. (2022). Ultrasensitive Ribo-seq reveals translational landscapes during mammalian oocyte-to-embryo transition and pre-implantation development. Nat. Cell Biol. *24*,

968–980. https://doi.org/10.1038/s41556-022-00928-6.

50. Hwang, J.Y., Jung, S., Kook, T.L., Rouchka, E.C., Bok, J., and Park, J.W. (2020). rMAPS2: an update of the RNA map analysis and plotting server for alternative splicing regulation. Nucleic Acids Res. *48*, W300–W306. https://doi.org/10.1093/nar/gkaa237.
51. Vitting-Seerup, K., and Sandelin, A. (2019). IsoformSwitchAnalyzeR: analysis of changes in genome-wide patterns of alternative splicing and its functional consequences. Bioinformatics *35*, 4469–4471. https://doi.org/10.1093/bioinformatics/btz247.
52. Li, B., and Dewey, C.N. (2011). RSEM: accurate transcript quantification from RNA-Seq data with or without a reference genome. BMC Bioinf. *12*, 323. https://doi.org/10.1186/1471-2105-12-323.
53. Wang, L., Park, H.J., Dasari, S., Wang, S., Kocher, J.-P., and Li, W. (2013). CPAT: Coding-Potential Assessment Tool using an alignment-free logistic regression model. Nucleic Acids Res. *41*, e74. https://doi.org/10.1093/nar/gkt006.
54. Wu, T., Hu, E., Xu, S., Chen, M., Guo, P., Dai, Z., Feng, T., Zhou, L., Tang, W., Zhan, L., et al. (2021). clusterProfiler 4.0: A universal enrichment tool for interpreting omics data. Innovation *2*, 100141. https://doi.org/10.1016/j.xinn.2021.100141.
55. Li, J., Pan, T., Chen, L., Wang, Q., Chang, Z., Zhou, W., Li, X., Xu, G., Li, X., Li, Y., and Zhang, Y. (2021). Alternative splicing perturbation landscape identifies RNA binding proteins as potential therapeutic targets in cancer. Mol. Ther. Nucleic Acids *24*, 792–806. https://doi.org/10.1016/j.omtn.2021.04.005.
56. Chen, S., Zhou, Y., Chen, Y., and Gu, J. (2018). fastp: an ultra-fast all-in-one FASTQ preprocessor. Bioinformatics *34*, i884–i890. https://doi.org/10.1093/bioinformatics/bty560.
57. Dobin, A., Davis, C.A., Schlesinger, F., Drenkow, J., Zaleski, C., Jha, S., Batut, P., Chaisson, M., and Gingeras, T.R. (2013). STAR: ultrafast universal RNA-seq aligner. Bioinformatics *29*, 15–21. https://doi.org/10.1093/bioinformatics/bts635.
58. Liao, Y., Smyth, G.K., and Shi, W. (2014). featureCounts: an efficient general purpose program for assigning sequence reads to genomic features. Bioinformatics *30*, 923–930. https://doi.org/10.1093/bioinformatics/btt656.
59. Shen, S., Park, J.W., Lu, Z.x., Lin, L., Henry, M.D., Wu, Y.N., Zhou, Q., and Xing, Y. (2014). rMATS: robust and flexible detection of differential alternative splicing from replicate RNA-Seq data. Proc. Natl. Acad. Sci. USA *111*, E5593–E5601. https://doi.org/10.1073/pnas.1419161111.
60. Zhou, Y., Zhou, B., Pache, L., Chang, M., Khodabakhshi, A.H., Tanaseichuk, O., Benner, C., and Chanda, S.K. (2019). Metascape provides a biologist-oriented resource for the analysis of systems-level datasets. Nat. Commun. *10*, 1523. https://doi.org/10.1038/s41467-019-09234-6.
61. Love, M.I., Huber, W., and Anders, S. (2014). Moderated estimation of fold change and dispersion for RNA-seq data with DESeq2. Genome Biol. *15*, 550. https://doi.org/10.1186/s13059-014-0550-8.
62. Kumar, L., and E Futschik, M. (2007). Mfuzz: a software package for soft clustering of microarray data. Bioinformation *2*, 5–7. https://doi.org/10.6026/97320630002005.
63. Durinck, S., Moreau, Y., Kasprzyk, A., Davis, S., De Moor, B., Brazma, A., and Huber, W. (2005). BioMart and Bioconductor: a powerful link between biological databases and microarray data analysis. Bioinformatics *21*, 3439–3440. https://doi.org/10.1093/bioinformatics/bti525.

STAR★METHODS

KEY RESOURCES TABLE

REAGENT or RESOURCE	SOURCE	IDENTIFIER
Chemicals, peptides, and recombinant proteins		
Pregnant mare serum gonadotrophin (PMSG)	Ningbo Second Hormone Factory	N/A
Human chorionic gonadotrophin (HCG)	Ningbo Second Hormone Factory	N/A
HTF *in Vitro* fertilization medium	Nanjing Aibei biotechnology	Cat# M1150
Mineral oil	Sigma	Cat# M8410
KSOM embryo culture media	Nanjing Aibei biotechnology	Cat# M1430
DMEM	Bio-Channel	Cat# BC-M-005
Fetal bovine serum	HyClone	Cat# SV30160.03
Penicillin-Streptomycin Solution	Biosharp	Cat# BL505A
Opti-MEM	Invitrogen	Cat# 31985070
Critical commercial assays		
HiPure Total RNA Micro Kit	Magen	Cat# R4114-01
HiScript III All-in-one RT SuperMix Kit	Vazyme	Cat# R333-01
2X Taq Plus Master Mix II	Vazyme	Cat# P213-02
HiPerFect Transfection Reagent	QIAGEN	Cat# 301705
Taq Pro Universal SYBR qPCR Master Mix	Vazyme	Cat# Q712
Deposited data		
Single-cell transcriptome data of human and mouse oocytes and preimplantation embryos	Gene Expression Omnibus (GEO)	GEO: GSE44183
Mouse oocyte and early embryo Ribo-lite and mRNA-seq	Gene Expression Omnibus (GEO)	GEO: GSE165782
Human oocyte and early embryo Ribo-lite and mRNA-seq	Gene Expression Omnibus (GEO)	GEO: GSE197265
RNA-Seq of Eif4a3 knockdown embryos	This paper	GEO: GSE247316
siRNA sequences for gene knockdown	See Table S4	N/A
qPCR primers for siRNA knockdown efficiency validation	See Table S5	N/A
PCR primers for differential alternative splicing events validation	See Table S6	N/A
Software and algorithms		
FastQC (version 0.11.9)	N/A	https://www.bioinformatics.babraham.ac.uk/projects/fastqc/
fastp (version 0.20.1)	Chen et al.,[56]	https://github.com/OpenGene/fastp
STAR (version 2.7.6a)	Dobin et al.,[57]	https://github.com/alexdobin/STAR
RSEM (version 1.3.3)	Li et al.,[52]	http://deweylab.biostat.wisc.edu/rsem
featureCounts (version 2.0.1)	Liao et al.,[58]	https://subread.sourceforge.net/featureCounts.html
rMATS (version 4.1.0)	Shen et al.,[59]	https://github.com/Xinglab/rmats-turbo
rmats2sashimiplot (version 2.0.2)	N/A	https://github.com/Xinglab/rmats2sashimiplot
rMAPS2	Hwang et al.,[50]	http://rmaps.cecsresearch.org/
Metascape database	Zhou et al.,[60]	https://metascape.org/gp/index.html#/main/step1

(*Continued on next page*)

Continued

REAGENT or RESOURCE	SOURCE	IDENTIFIER
R (version 4.1.1)	N/A	https://www.R-project.org/
DESeq2 package for R (version 1.34.0)	Love et al.,[61]	https://www.bioconductor.org/packages/release/bioc/html/DESeq2.html
Mfuzz package for R (version 2.54.0)	Kumar et al.,[62]	https://www.bioconductor.org/packages/release/bioc/html/Mfuzz.html
IsoformSwitchAnalyzeR package for R (version 1.16.0)	Vitting-Seerup et al.,[51]	https://www.bioconductor.org/packages/release/bioc/html/IsoformSwitchAnalyzeR.html
clusterProfiler package for R (version 4.2.2)	Wu et al.,[54]	https://www.bioconductor.org/packages/release/bioc/html/clusterProfiler.html
ggplot2 package for R (version 3.4.3)	N/A	https://cran.r-project.org/web/packages/ggplot2/index.html
biomaRt package for R (version 2.50.3)	Durinck et al.,[63]	https://www.bioconductor.org/packages/release/bioc/html/biomaRt.html

RESOURCE AVAILABILITY

Lead contact

Further information and requests for resources and reagents should be directed to and will be fulfilled by the lead contact, Ruizhi Feng (ruizhifeng@njmu.edu.cn).

Materials availability

This study did not generate new unique reagents.

Data and code availability

RNA-Seq data of Eif4a3-knockdown embryos in this study have been deposited to Gene Expression Omnibus (GEO) dataset. Accession numbers are listed in the key resources table. This paper does not report original code. Any additional information required to reanalyze the data reported in this paper is available from the lead contact upon request.

EXPERIMENTAL MODEL AND STUDY PARTICIPANT

Mice and ethics

ICR mice were purchased and housed in the animal facility at Nanjing Medical University. All animal protocols were approved by the Committee of Laboratory Animals and the Animal Care and Use Committee of Nanjing Medical University. Mice were maintained under a 12/12-hour-light cycle at 22°C with free access to food and water.

Culture and collection of mouse embryos

Female ICR mice (5–8 weeks) were super-ovulated by intraperitoneal injection of 7.5 IU of pregnant mare serum gonadotrophin (Ningbo Second Hormone Factory, China). After 46–48 h, the mice were injected with 7.5 IU of human chorionic gonadotrophin (Ningbo Second Hormone Factory, China). Ovulated metaphase II (MII) oocytes were collected 14–16 h later from the ampullae of oviducts and placed in HTF *in vitro* Fertilization Medium (Nanjing Aibei biotechnology, China, Cat#M1150). Sperm derived from F1 male mice of 10 weeks to 10 months (DBA and B6 hybrid F1 generation) and pre-incubated in HTF for 1 h under mineral oil (Sigma, USA, Cat#M5410) cover at 37°C with 5% of CO_2. After fertilization, the zygotes (Day1, D1) were washed and transferred into warmed KSOM embryo culture media (Nanjing Aibei biotechnology, China, Cat#M1430). We observed these embryos at each stage for 24 h (Day2, D2), 48 h (Day3, D3), 72 h (Day4, D4), 96 h (Day5, D5).

Gene knockdown by siRNA microinjection

Effective siRNAs at a concentration of 100 μM were microinjected to knock down the expression of target genes in mouse zygotes. Subsequently, these zygotes were transferred to KSOM culture medium and incubated them at 37°C, with 5% CO_2 in the air. We then observed the development of these embryos separately. siRNA sequences targeting specific genes were purchased from Tsingke Biotechnology and evaluated their knockdown efficiency in Neuro-2a cell line which was a gift from Xinuo Li at China Pharmaceutical University. To test the knockdown efficiency, we seeded Neuro-2a cells in 24-well plates (1*105 cells/well) in DEME (Bio-Channel, China, Cat#BC-*M*-005) supplemented with 10% fetal bovine serum (HyClone, USA, Cat#SV30160.03) and 10% Penicillin-Streptomycin Solution (Biosharp, China, Cat#BL505A), then incubated them at 37°C in an atmosphere of 5% CO2. After culturing Neuro-2a cell line for 24 h, we added 3 μL of HiPerFect Transfection Reagent (QIAGEN, USA, Cat#01705) with 50 μL of Opti-MEM (Invitrogen, USA, Cat#31985070) and 100 pmol of siRNA with 50 μL of Opti-MEM to

transfect these siRNAs into Neuro-2a cell line. Following transfection, we extracted RNA and reverse transcribed them to cDNA as described before. qRT-PCR (quantitative real-time PCR) was performed using Taq Pro Universal SYBR qPCR Master Mix (Vazyme, China, Cat#Q712) on a Step One Real-Time PCR System (Applied Biosystems, USA). For detailed effective siRNA sequences, refer to Table S4, and for the qPCR primer sequences, refer to Table S5.

METHOD DETAILS

Transcriptome data analysis

We downloaded the single-cell transcriptome data of human and mouse oocytes and preimplantation embryos with the accession number GEO: GSE44183. The human embryos cover seven consecutive stages of preimplantation development (oocyte, pronucleus, zygote, 2-cell, 4-cell, 8-cell, and morula) while mouse embryos cover six (oocyte, pronucleus, 2-cell, 4-cell, 8-cell, and morula). According to previous research,[48] we identified the pronucleus and zygote as the 1-cell stage.

Four human single-cell transcriptome data in 8-cell with an abnormal length of reads were discarded. Sequence quality control was performed by FastQC (version 0.11.9) and fastp (version 0.20.1). Subsequently, RNA-Seq reads were mapped to genome GRCm38/mm10 and GRCh37/hg19 respectively using STAR (version 2.7.6a). The bam files resulting from STAR were quantified by featureCounts (version 2.0.1) and the quantification file was further analyzed in software R (version 4.1.1). DESeq2 R package (version 1.34.0) was used to load count matrices and identify differentially expressed genes (DEGs) with padj<0.05 and $|\log_2 FoldChange|>2$.

R2-lite data analysis

mRNA-seq data and Ribo-lite data from previous research[1,49] were collected and analyzed. Translational efficiency (TE) was calculated by the ratio of Ribo-lite and mRNA-seq (FPKM+1/FPKM+1).

Temporal dynamic clustering analysis of gene expression profiles

Genes of different stages were clustered by Mfuzz R package, which can identify potential time-series patterns of expression profiles. Clusters of genes with similar patterns would help us understand the dynamic patterns of genes and how they are functionally linked. The membership values represent how well the gene is represented by the cluster, varying continuously from zero to one and color-encoded in the plot. We divided the genes into 22 clusters and chose 0.75 as the threshold to define the high relationships between genes within a cluster.

Differential alternative splicing events identification

Multivariate Analysis of Transcript Splicing for replicates (rMATS version 4.1.0) software was performed to detect differential alternative splicing events of two consecutive adjacent stages from RNA-Seq data with parameters: rmats.py –b1 stage1_path.txt –b2 stage2_path.txt –gtf gtf –od out –nthread 1 –readLength 90 -t paired –tmp_tmp. There are five types of alternative splicing events recognized by rMATS, namely skipped exon (SE), alternative 5′ splice site (A5SS), alternative 3′ splice site (A3SS), mutually exclusive exons (MXE) and retained intron (RI). The tool quantifies the expression of variable splicing events in different samples (with biological replicates) by rMATS statistical model and then calculates the p value by likelihood-ratio test to represent the difference between two groups of samples at Inclusion Level (IncLevel), also known as percent spliced-in (PSI). The FDR value was obtained by correcting the p value with the Benjamini&Hochberg algorithm. The difference of IncLevel (ΔIncLevel) is applied to evaluate the difference in the isoform ratio of a gene between two conditions. We filtered the output by $p < 0.05$, FDR <0.05 and $|\Delta IncLevel| > 0.1$ for subsequent analyses. Visualization of AS genes were exhibited by rmats2sashimiplot (version 2.0.2). rMAPS2 (RNA Map Analysis and Plotting Server 2, http://rmaps. cecsresearch.org/) was utilized to test for the enrichment of binding motifs and RNA binding proteins in the vicinity of alternatively spliced cassette exons in order to identify putative splicing regulators.[50]

Identification of isoform switch events

IsoformSwitchAnalyzeR package[51] was used to identify the expression of isoform switch events (ISEs) from RNA-Seq data via the quantitative results of transcripts obtained by RSEM (RNA-Seq by Expectation Maximization, version 1.3.3).[52] Besides, we integrate other annotations such as protein domains (via Pfam: https://www.ebi.ac.uk/Tools/pfa/pfamscan/), coding potential (via CPAT)[53] and sensitivity to Non-sense Mediated Decay (NMD) in ISEs' analysis.

Validation of differential alternative splicing events

RNA extraction from 2-cell and 4-cell embryos was performed using the HiPure Total RNA Micro Kit (Magen, Cat#R4114-01), and HiScript III All-in-one RT SuperMix Kit (Vazyme, Cat#R333-01) was used for cDNA. PCR was performed with 2X Taq Plus Master Mix II (Vazyme, Cat#P213-02), and the PCR primers are listed in Table S6. The PCR products were then separated on 1% agarose.

Function enrichment analysis

Gene Ontology enrichment analysis was performed using both clusterProfiler R package[54] and the Metascape database (https://metascape.org/gp/index.html#/main/step1). FDR less than 0.05 was chosen to represent significance. ggplot2 package was utilized to visualize the GO terms.

Prediction of DASEs-related RBP regulators

We collected 1,961 RBP genes in human from the Li et al.[55] study and matched these genes to mouse genome using biomaRt R package (version 2.48.3) to obtain the mouse RBP genes. In order to identify the RBPs that may potentially regulate the AS events in early embryonic development, we design a three-step pipeline that integrated RBP expression and AS profiling.

First, we identified DASEs between two consecutive stages. According to rMATS output file [AS_Events].MATS.JC.txt, we can collect the inclusion level values of specific splicing events for the specific stage. Next, we calculated the splicing event activity score. Since △IncLevel = IncLevel1 - IncLevel2, according to the parameters of rMATS, IncLevel1 was the evaluation of the previous developmental stage and IncLevel2 was the later one, we considered the events that contain an increase in the level of the spliceosome at the latter stage as splice active events (SA), and the events that contain a decrease in the level of the spliceosome at the latter stage as splice repressive events (SR). As a result, when △IncLevel >0, it is an SR event. For each stage j, the two scores were calculated as follows:

$$Splice(active)_j = \sum_{a=1}^{p} IncLevel_{aj}; if\ \triangle IncLevel_{aj} < 0$$

$$Splice(repressive)_j = \sum_{b=1}^{q} IncLevel_{bj}; if\ \triangle IncLevel_{bj} > 0$$

p and q are the number of AS events with $\triangle IncLevel$ less or greater than 0, respectively.

Second, we recognized differentially expressed RBPs between every two adjacent stages using Wilcoxon rank-sum test ($p < 0.05$). We hypothesized that the expression levels of RBPs could be correlated with the value of the inclusion level. Thus, we calculated the Spearman correlation coefficient between the expression level of RBPs and the inclusion level of splicing events. p.value <0.05 and absolute cor value >0.6 were selected for further analysis.

Smart-seq2 for Eif4a3-knockdown embryos

In order to explore the regulatory role of the RBP we predicted on alternative splicing, an experiment was carried out. Using effective siRNAs, Eif4a3 was selected as an example and its expression was decreased in mouse zygotes via microinjection. Blastocysts were collected on the fifth day, with 3 samples from each of the Negative Control group (NC) and the Eif4a3-knockdown (Eif4a3-KD) group, each sample containing 5 embryos. The embryos were then placed in SMART lysate and sent to LC-Bio Technologies (Hangzhou) Co., Ltd for Smart-seq2 sequencing, which was conducted using the Illumina Novaseq 6000 150PE platform.

QUANTIFICATION AND STATISTICAL ANALYSIS

All statistical analyses for experiments were performed with R (version 4.1.1) software. Number of replication and the standard error of mean (mean ± SEM) are outlined within each figure legend. Unpaired t-test was used in the comparison between NC and siRNA group. Each group were repeated at least three times to assure consistency. All statistics are *$p < 0.05$, **$p < 0.01$, ***$p < 0.001$, ****$p < 0.0001$.